Am J Physiol Endocrinol Metab
279: E1064–E1071, 2000.

Limitations to basal and insulin-stimulated skeletal muscle glucose uptake in the high-fat-fed rat

AMY E. HALSETH, DEANNA P. BRACY, AND DAVID H. WASSERMAN
Department of Molecular Physiology and Biophysics, Vanderbilt University School of Medicine, Nashville, Tennessee

Received 24 August 1999; accepted in final form 12 June 2000

Halseth, Amy E., Deanna P. Bracy, and David H. Wasserman. Limitations to basal and insulin-stimulated skeletal muscle glucose uptake in the high-fat-fed rat. *Am J Physiol Endocrinol Metab* 279: E1064–E1071, 2000.—Rats fed a high-fat diet display blunted insulin-stimulated skeletal muscle glucose uptake. It is not clear whether this is due solely to a defect in glucose transport, or if glucose delivery and phosphorylation are also impaired. To determine this, rats were fed standard chow (control rats) or a high-fat diet (HF rats) for 4 wk. Experiments were then performed on conscious rats under basal conditions or during hyperinsulinemic euglycemic clamps. Rats received primed constant infusions of 3-*O*-methyl-[^{3}H]glucose (3-*O*-MG) and [1-^{14}C]mannitol. Total muscle glucose concentration and the steady-state ratio of intracellular to extracellular 3-*O*-MG concentration [which distributes based on the transsarcolemmal glucose gradient (TSGG)] were used to calculate glucose concentrations at the inner and outer sarcolemmal surfaces ($[G]_{im}$ and $[G]_{om}$, respectively) in soleus. Total muscle glucose was also measured in two fast-twitch muscles. Muscle glucose uptake was markedly decreased in HF rats. In control rats, hyperinsulinemia resulted in a decrease in soleus TSGG compared with basal, due to increased $[G]_{im}$. In HF rats during hyperinsulinemia, $[G]_{im}$ also exceeded zero. Hyperinsulinemia also decreased muscle glucose in HF rats, implicating impaired glucose delivery. In conclusion, defects in extracellular and intracellular components of muscle glucose uptake are of major functional significance in this model of insulin resistance.

glucose delivery; glucose phosphorylation; 3-*O*-methylglucose; 2-deoxyglucose

IT IS WELL ESTABLISHED that dietary interventions in rodents are capable of significantly blunting insulin-stimulated glucose uptake by skeletal muscle (40). The question remains, however, as to the site or sites of functional limitations to muscle glucose uptake in vivo in this insulin-resistant state. A defect in glucose transport in dietary models of insulin resistance has been demonstrated numerous times (13, 27). There are reasons to believe that the other steps that comprise glucose uptake, delivery of glucose to the sarcolemma (15, 43), and glucose phosphorylation (38) may be impaired as well. One way to determine this is by assessing the magnitude of the transsarcolemmal glucose gradient (TSGG) in chow-fed and high-fat diet-fed (HF) rats under basal and insulin-stimulated conditions. Using a novel isotopic technique, we have previously demonstrated that physiological increments in insulin result in a narrowing of the TSGG in rat muscle, because the increase in sarcolemmal permeability is not accompanied by proportional increases in glucose delivery and/or phosphorylation (32). If the only defect in muscle glucose uptake in HF rats were at the glucose transport step, one would predict that the TSGG would exceed that seen in chow-fed rats during insulin stimulation. Therefore, we compared the maintenance of the TSGG under basal conditions and during a hyperinsulinemic euglycemic clamp in chow-fed (control) and HF rats by use of the glucose countertransport technique as has been described and applied previously (12, 32).

MATERIALS AND METHODS

Animal maintenance and surgical procedures. Male Sprague-Dawley rats (Sasco, Omaha, NE) were individually housed at 23°C on a 0600–1800 light cycle and allowed free access to water and food. Rats were divided into two groups: control rats, which were fed Purina Rodent Chow (65% of calories from carbohydrate, 11% from fat, 24% from protein), and HF rats, which were fed a high-fat diet (37% of calories from carbohydrate, 41% from fat, 22% from protein) obtained from Dr. Catherine Field, University of Alberta and as described previously (27). The fat content of this diet, although comparable with that found in the typical human diet, is sufficient to induce a significant degree of insulin resistance in the rat. The rats were housed under these conditions for ~3 wk, by which time their weights had reached 250–300 g. During this period, the food conversion index (FCI; weight gained/food consumed) for each rat was calculated. Catheters were inserted under anesthesia in the left common carotid artery and the right jugular vein (12). After surgery, animal weights and food intake were monitored daily, and only animals in which presurgery weight and FCI were restored were used for experiments (≥5 days). All procedures were preapproved by the Vanderbilt University Animal Care and Use Subcommittee and followed National Institutes of Health guidelines for the care and use of laboratory animals.

Experimental procedures. Food was removed from control and HF rats ~5 h before the beginning of a study. Rats were

Address for reprint requests and other correspondence: A. Halseth, Pharmacia Corporation, 800 N. Lindbergh Blvd., Mail Zone T1G, St. Louis, MO 63117.

The costs of publication of this article were defrayed in part by the payment of page charges. The article must therefore be hereby marked "*advertisement*" in accordance with 18 U.S.C. Section 1734 solely to indicate this fact.

studied either under basal conditions or during a hyperinsulinemic euglycemic clamp. At $t = -100$ min, an infusion of saline or insulin (1.0 mU·kg^{-1}·min^{-1}) was begun. Also at $t = -100$ min, primed infusions of [1-^{14}C]mannitol ([^{14}C]MN; 3.5 μCi primer and 60 nCi/min infusion) and 3-*O*-methyl-[^{3}H]glucose (3-*O*-MG; 25 μCi primer and 150 nCi/min infusion) were initiated. 3-*O*-MG is a substrate for glucose transport but is not further metabolized in skeletal muscle, whereas [^{14}C]MN is restricted to the extracellular space and thus can be used to measure this space. From $t = 0$ to 40 min, a constant-rate infusion of 2-[1,2-^{3}H]deoxyglucose (2-DG; 900 nCi/min) was given. 2-DG is transported into the cell and phosphorylated, yielding 2-DG-6-phosphate (2-DG-6-*P*). This 2-DG-6-*P* can undergo further metabolism to yield small amounts of other radiolabeled phosphorylated metabolites and glycogen. All radioisotopes were obtained from New England Nuclear (Boston, MA). Arterial blood samples ranging from 150 to 500 μl for tracer and/or insulin analyses were taken at −100, −70, −40, −10, 1, 2.5, 5, 7.5, 10, 15, 20, 25, 30, and 40 min. Washed erythrocytes from the experimental animal and whole blood from a donor rat were used to maintain hematocrit, but neither was infused after −10 min. On average, hematocrit fell from 42 to 37 by the end of the experiments, with no significant differences between groups. At 40 min, rats were anesthetized with intravenous pentobarbital sodium, and the soleus (comprised of slow-twitch oxidative fibers), gastrocnemius (gastroc; comprised of fast-twitch oxidative and fast-twitch glycolytic fibers), and superficial vastus lateralis (vastus; comprised of fast-twitch glycolytic fibers) muscles were rapidly excised and frozen in liquid N_2 within 10 s of removal from the animal. In separate basal experiments in which the equilibration period was extended to 300 min, soleus muscle [^{14}C]MN and 3-*O*-MG contents did not differ from those in the 140-min basal experiments, indicating that steady-state conditions were attained (data not shown). The 100-min isotope equilibration period used in these experiments was not long enough to reach steady-state conditions in the gastroc and vastus muscles, because the 3-*O*-MG content in muscle was higher when the equilibration period was extended to 300 min (12). Therefore, only data not dependent on 3-*O*-MG equilibration are presented for the gastroc and vastus muscles.

Processing of blood and muscle samples. Plasma glucose concentrations were measured by the glucose oxidase method with the use of an automated glucose analyzer (Beckman Instruments, Fullerton, CA), and immunoreactive insulin was measured using a double antibody method (29). Methods used to distinguish radioactivity from [^{14}C]MN, 3-*O*-MG, and 2-DG in muscle and plasma have been described previously (12). Briefly, the glucose analogs were distinguished on the basis of on whether or not they were precipitated with $Ba(OH)_2$ and $ZnSO_4$ and phosphorylated by yeast hexokinase (~10 units/sample). Tests in our laboratory revealed that treatment of samples with 10 units of hexokinase resulted in phosphorylation of ~25% of the 3-*O*-MG. Because both muscle and plasma samples were similarly affected, this did not change the calculated value of the steady-state ratio of 3-*O*-MG concentration in intracellular to extracellular water. One advantage of using $Ba(OH)_2$ and $ZnSO_4$ precipitation over the anion exchange method of separation (22) is that any 2-DG-6-phosphate (2-DG-6-*P*) incorporated into muscle glycogen (5, 42) will be counted in the same fraction as free 2-DG-6-*P* (12). This is due to the fact that all phosphorylated products of 2-DG as well as glycogen are recovered in the $Ba(OH)_2$ and $ZnSO_4$ precipitate (12). Muscle was deproteinized by homogenization in ice-cold 0.5% perchloric acid (PCA) and centrifuged at 4°C to remove insoluble proteins, and supernatants were kept on ice until neutralization with 5 M KOH. We have demonstrated in tests in our laboratory that, under these conditions, 2-DG-1-phosphate is preserved in its phosphorylated form instead of being degraded to 2-DG, as occurs in more concentrated PCA (7). The use of 0.5% PCA, therefore, prevents an overestimate of free 2-DG. Tests in our laboratory also showed that this concentration of PCA is also sufficient to prevent metabolism of glucose and 2-DG/2-DG-6-*P* by the muscle homogenate. Tissue glucose was measured in neutralized PCA extracts by an enzymatic method (28) and is expressed as millimoles per liter of muscle water, with a muscle water content of 0.75 ml/g used for all calculations. Nonesterified fatty acid (NEFA) concentration in plasma was determined spectrophotometrically using an automated analyzer (Monarch 2000 Centrifugal Analyzer, Instrumentation Laboratory, Lexington, MA) and a kit obtained from Wako Chemicals (NEFA-C, Richmond, VA).

Calculations. The fraction of extracellular to total water space in biopsies (F_e) was calculated with [^{14}C]MN as described previously (12). An index of muscle glucose uptake (R_g) (22) was calculated from muscle accumulation of 2-DG-6-*P* and other phosphorylated 2-DG metabolites and glycogen, the integrated plasma 2-DG concentration over the infusion period, and the plasma glucose concentration.

In these experiments, the steady state ratio of 3-O-MG concentration in intracellular to extracellular water (S_i/S_o), was determined to calculate the glucose concentration at the outer face of the sarcolemma ($[G]_{om}$), the glucose concentration at the inner face of the sarcolemma ($[G]_{im}$), and the TSGG, as has been described previously (12). S_i/S_o is calculated by the equation

$$S_i/S_o = ([3\text{-}O\text{-MG}]_m - [3\text{-}O\text{-MG}]_p \cdot F_e)/((1 - F_e) \cdot [3\text{-}O\text{-MG}]_p) \quad (1)$$

where the subscripts *m* and *p* refer to muscle and arterial plasma. Because 3-*O*-MG is not metabolized by muscle, extracellular gradients and intracellular gradients of this analog do not exist at steady state, and $[3\text{-}O\text{-MG}]_p$ equals the interstitial 3-*O*-MG concentration. S_i/S_o can be used to calculate the TSGG, because the steady-state distribution of 3-*O*-MG across the sarcolemma is determined by competition between glucose and 3-*O*-MG for binding sites on the transporters they share. The relationship between S_i/S_o and the TSGG is defined by the equation

$$S_i/S_o = (K_m + [G]_{im})/(K_m + [G]_{om}) \quad (2)$$

where K_m is the Michaelis-Menten constant for glucose transport. This equation has been described and applied previously (6, 10, 12, 30, 32). Assumptions of the method have been discussed in detail (10, 32).

Knowledge of S_i/S_o tells us the relationship between $[G]_{om}$ and $[G]_{im}$, but not the actual values for each of these concentrations. Because of the presence of glucose gradients, it is impossible to directly measure the true glucose concentration at the sarcolemma or anywhere in the interstitial or intracellular space. Therefore, we have developed a novel approach for calculating limits for the average $[G]_{om}$, based on two theoretical glucose distributions. In the first calculation of $[G]_{om}$, $[G]_{im}$ is assumed to be localized to such a small volume of the intracellular water that it contributes only negligibly to the total muscle glucose mass (denoted with superscript α). The second approach for the calculation of the mean $[G]_{om}$ assumes that $[G]_{im}$ is distributed evenly throughout the intracellular water (denoted with superscript β). Neither of these calculated values, or any other single value, will be identical to the actual $[G]_{om}$ at all places along

Table 1. *Arterial plasma glucose concentration, insulin concentration, and glucose infusion rate*

	Glucose, mM	Insulin, μU/ml	Glucose Infusion, $\mu mol \cdot kg^{-1} \cdot min^{-1}$
Control basal	7.6 ± 0.3	35 ± 6	—
Control insulin	8.0 ± 0.3	76 ± 11*	110 ± 9*
High-fat basal	7.3 ± 0.1	40 ± 4	—
High-fat insulin	7.9 ± 0.2*	69 ± 8*	34 ± 3*†

Data represent means ± SE; n = 7, 8, 6, and 8 for control basal, control insulin, high-fat-fed basal, and high-fat-fed insulin, respectively. *Significant differences from basal within a dietary treatment; †significant differences from control within an experimental treatment.

the sarcolemma; however, the current approach allows us to express the mean of these values within a known range. $[G]^{\alpha}_{om}$ was calculated as

$$[G]^{\alpha}_{om} = [G]_m/F_e \quad (3)$$

where $[G]_m$ is the muscle glucose concentration, and F_e is the fraction of muscle water that is extracellular. $[G]^{\alpha}_{im}$ was then calculated from *Eq. 2*. $[G]^{\beta}_{om}$ was calculated as

$$[G]^{\beta}_{om} = [[G]_m - [G]^{\beta}_{im} \cdot (1 - F_e)]/F_e \quad (4)$$

The solution to *Eq. 4* can be substituted into *Eq. 2* and then solved for $[G]^{\beta}_{im}$. $TSGG^{\alpha}$ and $TSGG^{\beta}$ are calculated with the values of $[G]^{\alpha}_{im}$ and $[G]^{\alpha}_{om}$, and $[G]^{\beta}_{im}$ and $[G]^{\beta}_{om}$, respectively

$$TSGG = [G]_{om} - [G]_{im} \quad (5)$$

A range of 2–5 mM has been reported for the K_m of GLUT-4 in vitro (33). A value of 3 mM was used in these calculations because it yielded a value for $[G]_{im}$ of ~0 under basal conditions, which is generally assumed to exist (e.g., Refs. 4, 9, 16), and because it approximates estimates obtained from muscle venous drainage in vivo (8, 45). Although the use of different values for K_m in calculations has a quantitative effect on the calculated data, no qualitative effects exist, and the magnitude of the quantitative differences decreases as S_i/S_o increases, which has been described in detail previously (32). It is notable that the K_m for muscle glucose transport is unchanged by insulin stimulation (11, 31, 35).

Statistical analyses. Statistical significance for variables with only one value was determined with one-factor ANOVA, using Fisher's PLSD as a post hoc test. For comparison of ranges defined by α- and β-boundaries ($[G]_{im}$, $[G]_{om}$, and TSGG), one-factor ANOVA was used to compare data sets consisting of both α- and β-values for each group. Also presented in the text in specific instances are P values for between-group comparisons (one-factor ANOVA) made between α- or β-values instead of entire ranges. We took this statistical approach so as not to exclude the possibility that either the α- or β-calculation is more representative of the actual distribution of glucose. Differences were considered statistically significant at $P < 0.05$. Data are expressed as means ± SE.

RESULTS

Animal characteristics. There were no differences between control and HF rats in body weight, 5-h-fasted arterial plasma glucose, or insulin concentrations (Table 1). Insulin concentrations were similarly elevated in control and HF rats by insulin infusion. The arterial plasma glucose concentration was maintained between 7.3 and 8.0 mM in all groups over the last 40 min of experiments. The glucose infusion rate necessary to maintain euglycemia during hyperinsulinemia was decreased ~70% in HF rats compared with control rats.

Arterial plasma nonesterified fatty acid concentration. At −100 min, plasma nonesterified fatty acid (NEFA) concentrations were not different between control (1.0 ± 0.1 mM) and HF (1.1 ± 0.1 mM) rats. NEFA concentrations were not altered by 140 min of saline infusion in control or HF rats. The response of plasma NEFAs to hyperinsulinemia differed between control and HF rats. In control rats, the plasma NEFA concentration decreased significantly to 0.6 ± 0.1 mM at 40 min, whereas the NEFA concentration was maintained in HF rats (1.4 ± 0.1 mM at 40 min; Fig. 1). This suggests that diet-induced insulin resistance is not limited to muscle glucose uptake but is also manifested by an inability of insulin to inhibit lipolysis at the adipocyte.

Muscle glucose concentration and R_g. Glucose concentrations in soleus and vastus were similar in control rats under basal and hyperinsulinemic conditions, but glucose concentration in gastroc fell in response to hyperinsulinemia ($P < 0.05$). Muscle glucose concentrations were not significantly different between HF and control rats in the basal state; however, during hyperinsulinemia, there was a significant decrease in glucose concentration in soleus and vastus in HF rats. R_g tended to be lower in HF rats under basal conditions, but this did not reach statistical significance. Under hyperinsulinemic conditions, R_g was significantly blunted in HF rats compared with control rats in all three muscles studied, indicating insulin resistance (Table 2). It is interesting to note that the falls in muscle glucose concentration in HF rats during hyperinsulinemia in soleus and vastus occurred despite the fact that the R_g values for these muscles were less than one-half of that measured in control rats; therefore, the fall is not due to greater glucose utilization.

Soleus S_i/S_o, $[G]_{om}$, $[G]_{im}$, and the TSGG. Soleus S_i/S_o, the ratio of 3-*O*-MG concentration in intracellu-

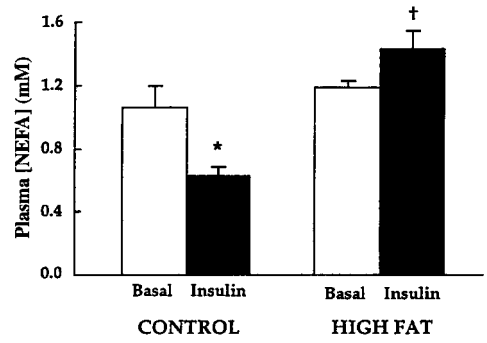

Fig. 1. Arterial plasma nonesterified fatty acid (NEFA) concentration (in mM) at the end of experiments in control and high-fat diet-fed (HF) rats under basal and hyperinsulinemic conditions. Data represent means ± SE; n = 7, 8, 6, and 8 for control basal, control insulin, HF basal and HF insulin, respectively. *Significant differences from basal within a dietary treatment; †significant differences from control within an experimental treatment.

Table 2. *Muscle glucose concentration and muscle R_g in soleus, gastroc and vastus*

	Muscle Glucose, mmol/l			R_g, μmol·100 g^{-1}·min^{-1}		
	Soleus	Gastroc	Vastus	Soleus	Gastroc	Vastus
Control basal	1.5 ± 0.1	1.5 ± 0.2	1.3 ± 0.1	15.4 ± 3.4	2.3 ± 0.7	1.2 ± 0.8
Control insulin	1.2 ± 0.1	1.2 ± 0.1*	1.1 ± 0.1	31.8 ± 3.5*	7.0 ± 1.0*	5.1 ± 0.6*
High-fat basal	1.6 ± 0.3	1.2 ± 0.1	1.3 ± 0.1	8.4 ± 2.2	1.0 ± 0.2	0.4 ± 0.2
High-fat insulin	0.8 ± 0.1*†	1.1 ± 0.1	1.0 ± 0.1*	14.4 ± 3.8†	3.2 ± 1.0*†	2.0 ± 0.5*†

Data represent means ± SE; n = 7, 8, 6, and 8 for control basal, control insulin, high-fat-fed basal, and high-fat-fed insulin, respectively. R_g, glucose uptake index; Gastroc, gastrocnemius; Vastus, superficial vastus lateralis. *Significant differences from basal within a dietary treatment; †significant differences from control within an experimental treatment.

lar to extracellular water, was 0.55 ± 0.13 in control rats in the basal state. This value was significantly ($P < 0.05$) increased to 0.79 ± 0.07 by hyperinsulinemia in control rats. In HF rats, soleus S_i/S_o in the basal state (0.82 ± 0.06) was significantly ($P < 0.05$) increased compared with that in control rats, indicating a narrower basal TSGG. In HF rats during hyperinsulinemia, S_i/S_o was 0.84 ± 0.09, which was not different from the S_i/S_o obtained in HF rats in the basal state or control rats during hyperinsulinemia.

In control rats studied in the basal state, the calculated range for soleus $[G]_{om}$ was between 3.6 ± 0.5 mM ($[G]^{\alpha}_{om}$) and 3.7 ± 0.8 mM ($[G]^{\beta}_{om}$), as shown in Fig. 1. Glucose concentration at the inner face of the membrane did not differ significantly from zero in this group, resulting in TSGG values that ranged between 3.1 ± 0.9 mM ($TSGG^{\alpha}$) and 3.6 ± 1.1 mM ($TSGG^{\beta}$) in control rats.

In control rats during hyperinsulinemia, the calculated range for soleus $[G]_{om}$ was not significantly different from that under basal conditions (Fig. 1). Soleus $[G]_{im}$ was significantly increased by hyperinsulinemia in these rats, with a calculated range between 2.3 ± 0.5 mM ($[G]^{\alpha}_{im}$) and 1.0 ± 0.2 mM ($[G]^{\beta}_{im}$). The increase in $[G]_{im}$ resulted in a significant decrease in the TSGG during hyperinsulinemia in control rats to values ranging between 1.9 ± 0.5 mM ($TSGG^{\alpha}$) and 1.2 ± 0.5 mM ($TSGG^{\beta}$; $P < 0.05$ compared with control rats under basal conditions).

When HF rats were studied under basal conditions, interpretation of results for $[G]_{om}$, $[G]_{im}$ and TSGG was dependent on whether the α- or β-condition was assumed to exist, because the range for these values was quite wide (Fig. 1). The entire range for soleus $[G]_{om}$ in HF rats in the basal state was not significantly different from the range in control rats under basal conditions. However, $[G]^{\beta}_{om}$ was significantly lower in HF than in control rats in the basal state ($P < 0.05$); so if the β-assumption more accurately represents the glucose distribution, glucose at the outer face of the sarcolemma may in fact be lower in HF than in control rats under these conditions. Regardless of assumptions regarding the distribution volume of glucose, $[G]_{im}$ in HF rats in the basal state was significantly increased compared with that in control rats. Consequently, the TSGG in HF rats under basal conditions was significantly decreased compared with that in control rats.

During hyperinsulinemia in HF rats, the entire range for soleus $[G]_{om}$ was unchanged compared with that for HF rats in the basal state (Fig. 2). In this case, however, $[G]^{\alpha}_{om}$ was significantly decreased by hyperinsulinemia in HF rats ($P < 0.005$). The range for $[G]_{im}$ was significantly decreased compared with the range for $[G]_{im}$ in HF rats under basal conditions and was similar to that calculated in control rats during hyperinsulinemia. The calculated range for TSGG in HF rats during hyperinsulinemia ranged between 1.8 ± 0.3 mM ($TSGG^{\alpha}$) to 1.0 ± 0.5 mM ($TSGG^{\beta}$), which was similar to the range of TSGG in HF rats in the basal state and in control rats during hyperinsulinemia.

Muscle water and muscle glucose to plasma glucose ratio. F_e, the fraction of muscle water that is extracellular, was significantly increased by hyperinsulinemia in control rats in soleus, but this was not observed in gastroc or vastus. F_e was not altered by hyperinsulinemia in HF rats in any muscle studied, nor was F_e different between control and HF rats in the basal state in any muscle studied (Table 3).

Also shown in Table 3 is muscle glucose normalized to the prevailing arterial plasma glucose concentration. By comparing F_e to the muscle glucose-to-plasma ratio, one can assess the extraction of glucose by the muscle, with a larger difference in these two percentages reflecting a lower average interstitial glucose concentration. The fact that F_e and the muscle-to-plasma glucose ratio are similar under basal conditions in gastroc and vastus indicates that no large gradient between the arterial plasma glucose concentration and the interstitial glucose concentration exists in these two fast-twitch muscles, in contrast to the situation in the soleus.

DISCUSSION

The consumption of a high-fat diet for ~4 wk resulted in a dramatic decrease in the ability of skeletal muscle to dispose of glucose, as has been demonstrated a number of times previously (23, 27). In this series of experiments, insulin-stimulated whole body glucose disposal was decreased by ~70% in HF rats, whereas muscle R_g was decreased by 50–70%. It has been demonstrated repeatedly that a defect in glucose transport exists in this model of insulin resistance (27, 37). Presumably, this occurs because of an impairment in insulin signaling to the GLUT-4-containing vesicles (44), because high-fat diet consumption has been demonstrated to impair both expression (20) and activation (44) of a number of insulin-signaling pathway constit-

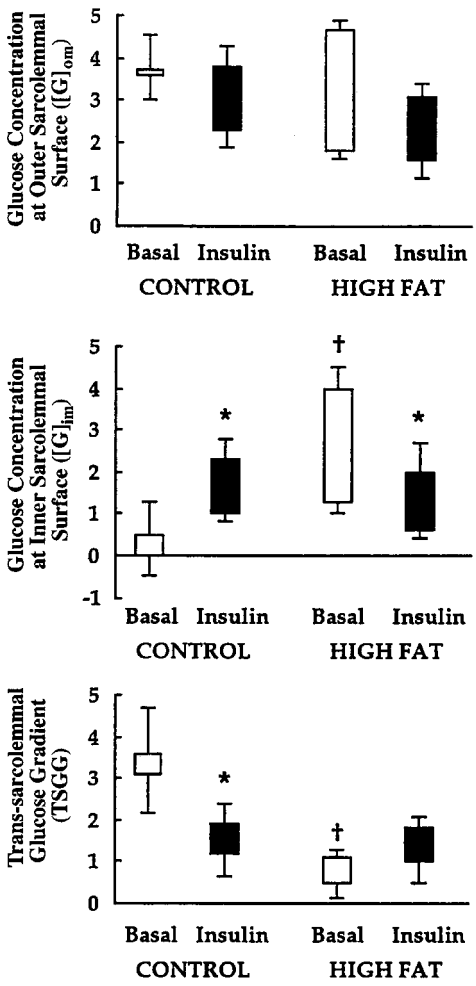

Fig. 2. Calculated glucose concentrations (in mM) at the outer and inner surfaces of the sarcolemma ($[G]_{om}$ and $[G]_{im}$, respectively) and the transsarcolemmal glucose gradient (TSGG) in soleus muscle from control and HF rats under basal and hyperinsulinemic conditions. Data represent means ± SE for the ranges bounded by α- and β-values; n = 7, 8, 6, and 8 for control basal, control insulin, HF basal, and HF insulin, respectively. The α- and β-values represent the top and bottom of each of the ranges, respectively, except for $[G]_{om}$ and TSGG in the control basal group, where the β-values are the upper limit. *Significant differences from basal within a dietary treatment; †significant differences from control within an experimental treatment.

uents. The data presented in this work provide evidence that a defect at the level of glucose transport is not the sole cause of this diet-induced insulin resistance but that pre- and posttransport steps also make significant functional contributions to this impairment.

Three muscles were studied in these experiments, one comprised almost solely of slow-twitch oxidative fibers (soleus), from which most of the results were obtained, and two muscles comprised primarily of fast-twitch fibers, the gastroc and vastus. This allowed for a first assessment of how diet-induced insulin resistance may affect specific types of muscle fibers. It is difficult to measure fiber-specific effects in humans, because most human muscles are comprised of a mixture of fiber types. One advantage of the rat model is that the soleus and superficial vastus lateralis are relatively homogeneous for fiber type; thus glucose gradients between arterial plasma and the sarcolemma should display less regional heterogeneity. A technical disadvantage to muscles comprised of fast-twitch fibers is that, presumably because of their decreased capillary density and perfusion, the isotope equilibration period used in these experiments was not of sufficient duration to reach steady-state conditions (see MATERIALS AND METHODS). Therefore, only analyses not dependent on 3-*O*-MG accumulation were performed on these muscles. Conclusions regarding the intracellular contribution to impaired muscle glucose uptake must be limited to the soleus. It should be noted that, because of its role as a postural muscle and its associated slow-twitch fiber type composition, the soleus is not necessarily representative of human muscle overall.

Data from all three muscles support an impairment in glucose delivery in HF rats. Despite the much lower rate of glucose flux in muscle from HF rats, all three muscles were characterized by a fall in the muscle glucose-to-plasma glucose ratio in response to hyperinsulinemia, which was apparent only in gastroc in control rats. It is possible that a structural or functional defect may exist within the microcirculation of HF rats, resulting in decreased muscle capillary perfusion. For example, a decrease in capillary density has been reported in insulin-resistant human (24, 26) and rat muscle after 6–8 wk of poorly controlled insulin-deficient diabetes (21). Another possibility is that there is a decrease in insulin-stimulated muscle blood flow in HF rats. Although the ability of insulin at physiological concentrations to stimulate muscle blood flow is con-

Table 3. *F_e and muscle glucose to plasma glucose ratio*

	F_e	Muscle [glucose]/ Plasma [glucose]
Soleus		
Control basal	0.34 ± 0.02	0.17 ± 0.04
Control insulin	0.39 ± 0.02*	0.20 ± 0.02
High-fat basal	0.30 ± 0.02	0.23 ± 0.03
High-fat insulin	0.28 ± 0.01†	0.11 ± 0.02*†
Gastrocnemius		
Control basal	0.23 ± 0.01	0.21 ± 0.02
Control insulin	0.30 ± 0.03	0.15 ± 0.01*
High-fat basal	0.20 ± 0.01	0.17 ± 0.01
High-fat insulin	0.19 ± 0.01†	0.14 ± 0.01*
Superficial Vastus Lateralis		
Control basal	0.22 ± 0.02	0.17 ± 0.02
Control insulin	0.22 ± 0.03	0.14 ± 0.02
High-fat basal	0.21 ± 0.01	0.18 ± 0.01
High-fat insulin	0.18 ± 0.01	0.12 ± 0.01*

Data represent means ± SE; n = 7, 8, 6, and 8 for control basal, control insulin, high-fat-fed basal, and high-fat-fed insulin, respectively. F_e, fraction of total muscle water that is extracellular. *Significant differences from basal within a dietary treatment; †significant differences from control within an experimental treatment.

troversial (1, 41), a significant amount of data demonstrates that insulin does have effects on arteriole resistance (15, 43). The fall in muscle glucose concentration with hyperinsulinemia in HF rats is consistent with the demonstration that insulin-induced arteriole vasodilation is impaired in two rat models of insulin resistance, the fructose-fed rat (15) and the genetically obese Zucker rat (43). In addition, in the spontaneously hypertensive rat, the ability of insulin to increase Doppler-measured hindlimb blood flow is blunted (34). It is therefore possible that insulin resistance of the vasculature, in which the insulin-stimulated increase in glucose delivery is blunted or prevented, is a contributor to the impairment in muscle glucose uptake.

Under basal conditions, the TSGG in the soleus was reduced in HF compared with control rats. The magnitude of the TSGG is directly related to the degree to which glucose transport limits glucose uptake. The fact that the TSGG was small in the soleus of HF rats under basal conditions means that the sarcolemma functions as less of a relative barrier to glucose uptake than it does in control rats. This does not necessarily mean that the sarcolemmal permeability is greater in HF than in control rats under these conditions; instead, it is more likely that the processes that maintain the TSGG (glucose delivery and/or glucose phosphorylation) are insufficient to maintain the larger TSGG observed in chow-fed rats. Because the distribution volume of glucose in intracellular water is unknown, $[G]_{om}$, $[G]_{im}$, and the TSGG were calculated on the basis of two theoretical distributions (referred to as α and β), as described in MATERIALS AND METHODS. Under conditions where both the S_i/S_o and the muscle glucose concentration are high, as was the case for the soleus in HF rats under basal conditions, the ranges spanned by the α- and β-values for $[G]_{om}$ and $[G]_{im}$ are wide. Thus precise conclusions regarding the roles of glucose delivery and glucose phosphorylation in limiting muscle glucose uptake cannot be determined. Regardless of these assumptions, however, $[G]_{im}$ was elevated in soleus in HF rats in the basal state, indicating a limitation at glucose phosphorylation.

In soleus muscle from both control and HF rats, hyperinsulinemia resulted in an increase in $[G]_{im}$ above zero. If the only defect in glucose uptake in HF rats occurred at the glucose transport step, one would predict that $[G]_{im}$ would be lower in HF than in control rats. Instead, it appears that glucose phosphorylation becomes limiting at a lower rate of glucose uptake in HF rats. An impairment in hexokinase II activity has been reported in muscle from insulin-resistant mice (3) and humans (25), but this has not been observed in high-fat diet-induced insulin resistance (17, 44) or muscle from obese Zucker rats (38). Even if hexokinase activity is normal in insulin-resistant muscle, the high sensitivity of hexokinase I and hexokinase II to inhibition by G-6-*P* means that a defect in utilization of G-6-*P* (either by incorporation into glycogen or by metabolism in glycolysis) may also explain the inability of phosphorylation in HF muscle to match pace with the rate of glucose transport. In support of this, there are some data suggesting that muscle G-6-*P* levels are higher in HF rats after a hyperinsulinemic clamp (18), and it has also been reported that hexokinase is more sensitive to inhibition by G-6-*P* in insulin-resistant muscle (38). This is clearly an area in which more work needs to be performed.

One interesting result from these experiments is that the fall in plasma NEFA concentration that normally occurs in response to hyperinsulinemia was not observed in HF rats. We view this as both a consequence of insulin resistance (i.e., insulin resistance at the adipocyte) and a possible contributing factor to the development of muscle insulin resistance in these rats. An acute infusion of a triglyceride emulsion designed to increase the plasma NEFA concentration is able to cause insulin resistance within ~2–4 h in humans (2, 36) and rats (14, 19). Acute NEFA elevation is also able to prevent endothelium-dependent increases in leg blood flow in humans (39). This could be a mechanism for the fall in the muscle glucose-to-plasma glucose ratio observed during hyperinsulinemia in HF rats in soleus, vastus, and gastroc. In addition, an acute elevation of NEFA concentration during a hyperinsulinemic clamp results in a rise in the muscle G-6-*P* concentration in rats (14), and may therefore relate to the impairment observed in glucose phosphorylation in soleus muscle from HF rats.

In conclusion, we have demonstrated that the impairment in muscle glucose uptake induced by consumption of a high-fat diet for ~4 wk is due not only to an impairment in glucose transport but also to defects in glucose delivery and glucose phosphorylation. In soleus muscle from HF rats, glucose phosphorylation is impaired in both the basal and insulin-stimulated state, whereas glucose delivery becomes more limiting to glucose uptake in soleus during hyperinsulinemia. In two muscles comprised of fast-twitch fibers, it appears that glucose delivery is a more important site of resistance to insulin-stimulated glucose uptake in HF rats than in control rats. Taken in total, these data and data from the literature suggest that the consumption of a high-fat diet affects each of the steps that comprise muscle glucose uptake. The phenotype of "skeletal muscle insulin resistance" is in fact due to defects at both muscle and the vasculature, which impair both the delivery and extraction of glucose.

The authors are grateful to Dr. Andrea Mari for insight in the preparation of the manuscript, and Dr. George Reed for assistance with statistical analyses.

This work was supported by NIH Grant RO1 DK-50277. A. Halseth was supported by Training Grant 5 T32 DK-07563–08.

REFERENCES

1. **Baron AD and Clark MG.** Role of blood flow in the regulation of muscle glucose uptake. *Annu Rev Nutr* 17: 487–499, 1997.
2. **Boden G, Jadali F, White J, Liang Y, Mozzoli M, Chen X, Coleman E, and Smith C.** Effects of fat on insulin-stimulated carbohydrate metabolism in normal men. *J Clin Invest* 88: 960–966, 1991.

3. **Braithwaite SS, Palazuk B, Colca JR, Edwards CW, and Hofmann C.** Reduced expression of hexokinase II in insulin-resistant diabetes. *Diabetes* 44: 43–48, 1995.
4. **Cline GW, Jucker BM, Trajanoski Z, Rennings AJM, and Shulman GI.** A novel ^{13}C NMR method to assess intracellular glucose concentration in muscle, in vivo. *Am J Physiol Endocrinol Metab* 274: E381–E389, 1998.
5. **Colwell DR, Higgins JA, and Denyer GS.** Incorporation of 2-deoxy-D-glucose into glycogen. Implications for measurement of tissue-specific glucose uptake and utilization. *Int J Biochem Cell Biol* 28: 115–121, 1996.
6. **Dienel GA, Cruz NF, Adachi K, Sokoloff L, and Holden JE.** Determination of local brain glucose level with [^{14}C]methylglucose: effects of glucose supply and demand. *Am J Physiol Endocrinol Metab* 273: E839–E849, 1997.
7. **Dienel GA, Cruz NF, Mori K, and Sokoloff L.** Acid lability of metabolites of 2-deoxyglucose in rat brain: implications for estimates of kinetic parameters of deoxyglucose phosphorylation and transport between blood and brain. *J Neurochem* 54: 1440–1448, 1990.
8. **Edelman SV, Laakso M, Wallace P, Brechtel G, Olefsky JM, and Baron AD.** Kinetics of insulin-mediated and non-insulin-mediated glucose uptake in humans. *Diabetes* 39: 955–964, 1990.
9. **Ferrannini E, Smith JD, Cobelli C, Toffolo G, Pilo A, and DeFronzo RA.** Effect of insulin on the distribution and disposition of glucose in man. *J Clin Invest* 76: 357–364, 1985.
10. **Foley JE, Cushman SW, and Salans LB.** Intracellular glucose concentration in small and large rat adipose cells. *Am J Physiol Endocrinol Metab* 238: E180–E185, 1980.
11. **Gottesman I, Mandarino L, Verdonk C, and Rizza R.** Insulin increases the maximal velocity for glucose uptake with altering the Michaelis constant in man: evidence that insulin increases glucose uptake merely by providing additional transport sites. *J Clin Invest* 70: 1310–1314, 1982.
12. **Halseth AE, Bracy DP, and Wasserman DH.** Limitations to exercise- and maximal insulin-stimulated muscle glucose uptake in vivo. *J Appl Physiol* 85: 2305–2313, 1998.
13. **Han DH, Hansen PA, Host HH, and Holloszy JO.** Insulin resistance of muscle glucose transport in rats fed a high-fat diet: a reevaluation. *Diabetes* 46: 1997.
14. **Jucker BM, Rennings AJM, Cline GW, and Shulman GI.** ^{13}C and ^{31}P NMR studies on the effects of increased plasma free fatty acids on intramuscular glucose metabolism in the awake rat. *J Biol Chem* 272: 10464–10473, 1997.
15. **Katakam PVG, Ujhelyi MR, Hoenig ME, and Miller AW.** Endothelial dysfunction precedes hypertension in diet-induced insulin resistance. *Am J Physiol Regulatory Integrative Comp Physiol* 275: R788–R792, 1998.
16. **Katz A, Nyomba BL, and Bogardus C.** No accumulation of glucose in human skeletal muscle during euglycemic hyperinsulinemia. *Am J Physiol Endocrinol Metab* 255: E942–E945, 1988.
17. **Kern M, Tapscott EB, Downes DL, Frisell WR, and Dohm GL.** Insulin resistance induced by high-fat feeding is only partially reversed by exercise training. *Pflügers Arch* 417: 79–83, 1990.
18. **Kim JK, Wi JK, and Youn JH.** Metabolic impairment precedes insulin resistance in skeletal muscle during high-fat feeding in rats. *Diabetes* 45: 651–658, 1996.
19. **Kim JK, Wi JK, and Youn JH.** Plasma free fatty acids decrease insulin-stimulated skeletal muscle glucose uptake by suppressing glycolysis in conscious rats. *Diabetes* 45: 446–453, 1996.
20. **Kim YB, Nakajima R, Matsuo T, Inoue T, Sekine T, Komuro M, Tamura T, Tokuyama K, and Suzuki M.** Gene expression of insulin signal-transduction pathway intermediates is lower in rats fed a beef tallow diet than in rats fed a safflower oil diet. *Metabolism* 45: 1080–1088, 1996.
21. **Kindig CA, Sexton WL, Fedde MR, and Poole DC.** Skeletal microcirculatory structure and hemodynamics in diabetes. *Respir Physiol* 111: 163–175, 1998.
22. **Kraegen EW, James DE, Jenkins AB, and Chisholm DJ.** Dose response curves for in vivo insulin sensitivity in individual tissues in rats. *Am J Physiol Endocrinol Metab* 248: E353–E362, 1985.
23. **Kraegen EW, James DE, Storlien LH, Burleigh KM, and Chisholm DJ.** In vivo insulin resistance in individual peripheral tissues of the high fat fed rat: assessment of euglycemic clamp plus deoxyglucose administration. *Diabetologia* 29: 192–199, 1986.
24. **Kriketos AD, Pan DA, Lillioja S, Cooney GJ, Baur LA, Milner MR, Sutton J, Jenkins AB, Bogardus C, and Storlien LH.** Interrelationships between muscle morphology, insulin action, and adiposity. *Am J Physiol Regulatory Integrative Comp Physiol* 270: R1332–R1339, 1996.
25. **Kruszynska YT, Mulford MI, Baloga J, Yu JG, and Olefsky JM.** Regulation of skeletal muscle hexokinase II by insulin in nondiabetic and NIDDM subjects. *Diabetes* 47: 1107–1113, 1998.
26. **Lillioja S, Young AA, Cutler CL, Ivy JL, Abbott WGH, Zawadzki JK, Yki-Järvinen H, Christin L, Secomb TW, and Bogardus C.** Skeletal muscle capillary density and fiber type are possible determinants of in vivo insulin resistance in man. *J Clin Invest* 80: 415–424, 1987.
27. **Liu S, Baracos VE, Quinney HA, Bricon TL, and Clandinin MT.** Parallel IGF-1 and insulin resistance in muscles of rats fed a high fat diet. *Endocrinology* 136: 3318–3324, 1995.
28. **Lloyd B, Burrin J, Smythe P, and Alberti KGMM.** Enzymatic fluorometric continuous-flow assays for blood glucose, lactate, pyruvate, alanine, glycerol, and 3-hydroxybutyrate. *Clin Chem* 24: 1724–1729, 1978.
29. **Morgan CR and Lazarow AL.** Immunoassay of insulin: two antibody system. Plasma insulin of normal, subdiabetic, and diabetic rats. *Am J Med Sci* 257: 415–419, 1963.
30. **Morgan HE, Regen DM, and Park CR.** Identification of a mobile carrier-mediated sugar transport system in muscle. *J Biol Chem* 239: 369–374, 1964.
31. **Nesher R, Karl I, and Kipnis D.** Dissociation of effects of insulin and contraction on glucose transport in rat epitrochlearis muscle. *Am J Physiol Cell Physiol* 249: C226–C232, 1985.
32. **O'Doherty RM, Halseth AE, Granner DK, Bracy DP, and Wasserman DH.** Analysis of insulin-stimulated skeletal muscle glucose uptake in the conscious rat using isotopic glucose analogues. *Am J Physiol Endocrinol Metab* 274: E287–E296, 1998.
33. **Olson AL and Pessin JE.** Structure, function, and regulation of the mammalian facilitative glucose transporter gene family. *Annu Rev Nutr* 16: 235–256, 1996.
34. **Pitre M, Nadeau A, and Bachelard H.** Insulin sensitivity and hemodynamic responses to insulin in Wistar-Kyoto and spontaneously hypertensive rats. *Am J Physiol Endocrinol Metab* 271: E658–E668, 1996.
35. **Rennie MJ, Idstrom JP, Mann GE, Schersten T, and Bylund-Fellinius AC.** A paired-tracer dilution method for characterizing membrane transport in the perfused rat hindlimb. *Biochem J* 214: 737–743, 1983.
36. **Roden M, Price TB, Perseghin G, Falk KP, Rothman DL, Cline GW, and Shulman GI.** Mechanism of free fatty acid-induced insulin resistance in humans. *J Clin Invest* 97: 2859–2865, 1996.
37. **Rosholt MN, King PA, and Horton ES.** High-fat diet reduces glucose transporter responses to both insulin and exercise. *Am J Physiol Regulatory Integrative Comp Physiol* 266: R95–R101, 1994.
38. **Sanderson AL, Radda GK, and Leighton B.** Abnormal regulation of hexokinase in insulin-resistant skeletal muscle. *Biochem Mol Med* 59: 80–86, 1996.
39. **Steinberg HO, Tarshoby M, Monestel R, Hook G, Cronin J, Johnson A, Bayazeed B, and Baron AD.** Elevated circulating free fatty acid levels impair endothelium-dependent vasodilation. *J Clin Invest* 100: 1230–1239, 1997.
40. **Storlien LH, Baur LA, Kriketos AD, Pan DA, Cooney GJ, Jenkins AB, Calvert GD, and Campbell LV.** Dietary fats and insulin action. *Diabetologia* 39: 621–631, 1996.
41. **Utriainen T, Malmstrom R, Makimattila S, and Yki-Järvinen H.** Methodological aspects, dose-response characteristics, and causes of interindividual variation in insulin stimulation of limb blood flow in normal subjects. *Diabetologia* 38: 555–564, 1995.
42. **Virkamaki A, Rissanen E, Hamalainen S, Utriainen T, and Yki-Järvinen H.** Incorporation of [3-^{3}H]glucose and 2-[1-

[14]C]deoxyglucose into glycogen in heart and skeletal muscle in vivo: implications for the quantitation of tissue glucose uptake. *Diabetes* 46: 1106–1110, 1997.

43. **Walker AB, Dores J, Buckingham RE, Savage MW, and Williams G.** Impaired insulin-induced attenuation of noradrenaline-mediated vasoconstriction in insulin-resistant obese Zucker rats. *Clin Sci (Colch)* 93: 235–241, 1997.
44. **Zierath JR, Houseknecht KL, Gnudi L, and Kahn BB.** High-fat feeding impairs insulin-stimulated GLUT4 recruitment via an early insulin-signaling defect. *Diabetes* 46: 215–223, 1997.
45. **Zinker BA, Bracy D, Lacy DB, Jacobs J, and Wasserman DH.** Regulation of glucose uptake and metabolism during exercise: an in vivo analysis. *Diabetes* 42: 956–965, 1993.